Electron and ion transmission of the gating foil for the TPC in the ILC experiment

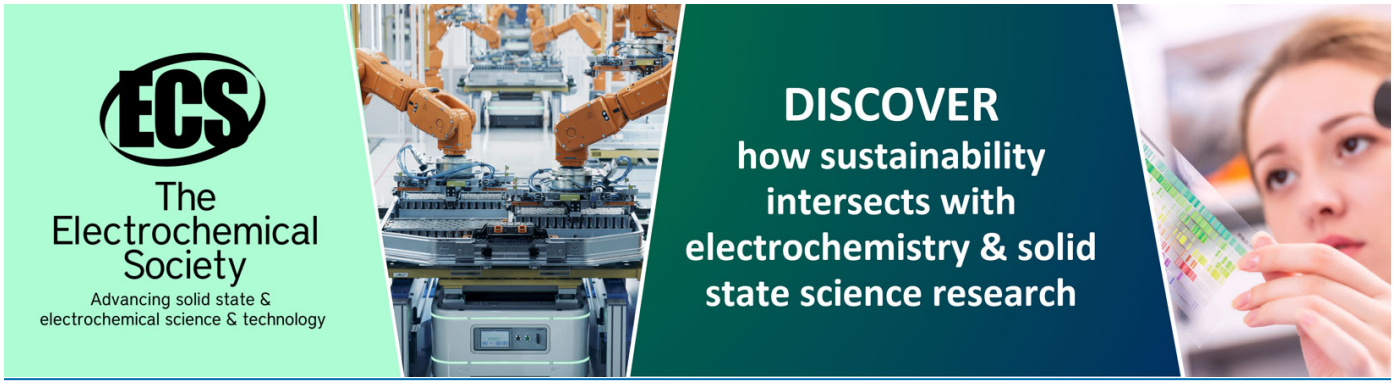

Journal of Physics: Conference Series **1498** (2020) 012020 doi:10.1088/1742-6596/1498/1/012020

Electron and ion transmission of the gating foil for the TPC in the ILC experiment

M Kobayashi[1], T Ogawa[2], A Shoji[3], Y Aoki[2], K Ikematsu[4,13], P Gros[4,14] T Kawaguchi[5], D Arai[6], M Iwamura[6], K Katsuki[6], A Koto[6], M Yoshikai[6], K Fujii[1], T Fusayasu[4], Y Kato[7] , S Kawada[8], T Matsuda[1], S Narita[3], K Negishi[3], H Qi[9], R D Settles[10], A Sugiyama[4], T Takahashi[5], J Tian[1,15], T Watanabe[11] and R Yonamine[12]

[1]High Energy Accelerator Research Organization (KEK), Tsukuba 305-0801, Japan
[2]The Graduate University for Advanced Studies (Sokendai), Tsukuba 305-0801, Japan
[3]Iwate University, Iwate 020-8551, Japan
[4]Saga University, Saga 840-8502, Japan
[5]Hiroshima University, Higashi-Hiroshima 739-8530, Japan
[6]Fujikura Ltd., 1440, Mutsuzaki, Sakura-city, Chiba 285-8550, Japan
[7]Kindai University, Higashi-Osaka 577-8502, Japan
[8]Deutsches Elektronen-Synchrotron (DESY), D-22607 Hamburg, Germany
[9]Institute of High Energy Physics, Chinese Academy of Sciences, Beijing 100049, China
[10]Max Planck Institute for Physics, DE-80805 Munich, Germany
[11]Kogakuin University, Shinjuku 163-8677, Japan
[12]Department of Physics, Tohoku University, Sendai 980-8578, Japan

E-mail: kobayasi@post.kek.jp

Abstract.

We have developed a gating foil for the time projection chamber envisaged as a central tracker for the international linear collider experiment. It has a structure similar to the Gas Electron Multiplier (GEM) with a higher optical aperture ratio and functions as an ion gate without gas amplification. The transmission rate for electrons was measured in a counting mode for a wide range of the voltages applied across the foil using an ^{55}Fe source and a laser in the absence of a magnetic field. The upper limit of the transmission rate for positive ions was estimated to be 3.36 ± 0.05 (stat. only)) $\times 10^{-4}$ from the measured electron transmission at a relatively low reverse bias voltage applied to the foil ($\Delta V = -15.5$ V). The blocking power of the gating foil was confirmed to be high enough to suppress the influence of ion backflow.

1. Introduction

We are designing a time projection chamber (TPC) [1] using gas electron multipliers (GEMs) [2] or Micromegas [3] for the central tracker of the international large detector (ILD) [4]

[13] Present address: Institute of Multidisciplinary Research for Advanced Materials (IMRAM), Tohoku University, Sendai 980-8577, Japan.
[14] Present address: Department of Physics, Engineering Physics & Astronomy, Queen's University, Kingston, Ontario K7L 3N6, Canada.
[15] Present address: ICEPP, University of Tokyo, Hongo, Tokyo 113-0033, Japan.

for the future international linear collider (ILC) experiment [5]. A high momentum resolution of $\sigma_{P_\mathrm{t}}/P_\mathrm{t} \sim 10^{-4} \cdot P_\mathrm{t}$ [GeV/c] is required of the ILD-TPC alone under an axial magnetic field of ~ 3.5 T. In order to fulfill the requirement within the space available for the TPC, each readout pad row with a height of 5 – 6 mm needs to have azimuthal spatial resolution of $\lesssim$ 100 µm for stiff radial tracks throughout the entire sensitive volume.

It is difficult to achieve such high spatial resolution in a strong magnetic field with conventional readout modules (sectors) equipped with a multi-wire proportional chamber (MWPC) due to the so-called $E \times B$ effect near the wire planes [6]. Among micro-pattern gas detectors (MPGDs), which are virtually free from the $E \times B$ effect as well as from the angular wire effect, our group (ILD-TPC Asia) has chosen GEM as a gas amplification device to be operated in an appropriate gas mixture because of the natural charge spread in its stack during gas multiplication.

The spatial resolution of around 100 µm seems feasible with a gas mixture of Ar-CF_4(3%)-isobutane(2%) [7–9]. The major remaining issue to be addressed is the influence of positive ions accumulated in the drift volume of the TPC. The positive ions disturb the otherwise uniform drift field and distort the reconstructed tracks.

The ILC machine has a peculiar time structure of the beam crossings. The electron and positron beams are both a train of 1312 bunches, 554 nsec apart in time (baseline design), and collide every 200 msec with a duration of $\lesssim$ 1 msec [10]. According to the estimation based on a simulated beam background [11], the influence of primary ions is expected to be small, whereas that of secondary ions created in the gas amplification is not acceptable [4]. The secondary ions form a $\sim$ 3-mm-thick disk above the gas amplification device just after each beam (bunch-train) crossing. The ion disk then slowly drifts back towards the central membrane with small diffusion. As a result, 3 – 4 ion disks ($\sim$ 75 cm apart, depending on the drift field and the mobility of positive ions) co-exist in the drift volume at the end of every beam crossing.

The fractional ion backflow of the gas amplification device (IBF) is often defined as the average ratio of the number of outgoing positive ions to the number of amplified electrons reaching the readout pad plane for a single incoming drift electron. The maximum azimuthal displacement caused by positive ions is estimated to be $\mathcal{O}(1$ mm) with the planned effective gas gain of 2000 and the value of IBF of $\lesssim 5\%$ for our present double-GEM configuration.

We plan to operate the TPC in a *semi-continuous* mode with a gating plane, exploiting the beam timing structure mentioned above, in order to prevent the secondary ions from entering the drift volume while keeping it fully active during the beam collisions. The gating plane is placed $\lesssim$ 10 mm above the gas amplification device. The gate remains open during the beam crossing and is closed after collecting all the drift electrons. The back-drifting ions are almost completely trapped by the gating plane within several milliseconds after its closure. The gate is then re-opened prior to the next beam crossing. As a consequence, there are no ion disks at the beginning of each beam crossing.

Inspired by the work by F. Sauli and coworkers [12] we have developed a gating plane without wires after a detailed simulation study [13] and experiments with small prototypes [14]. It has a thin GEM-like structure with a large optical aperture ratio, but is operated without gas amplification. The large aperture ratio is required to ensure good electron *collection efficiency* under a high axial magnetic field while the thin insulator (polyimide) is favorable to reduce the possibility for drift electrons in the hole to be (temporarily) trapped on its inner wall.

It is essentially a precisely aligned double-mesh layer with an embedded insulating spacer in-between, to be referred to as the gating foil hereafter in the present paper. The gating foil with a frame can be mounted on top of the amplification GEM stack or Micromegas, just like an additional ordinary GEM foil, thereby realizing a *wire-less* gas amplification device for TPCs with ion-blocking capability.

In addition to the high blocking capability against positive ions at the closed state, the

gating foil is required to have high transparency of $\gtrsim 80\%$ for drift electrons at the open state in order not to compromise appreciably the azimuthal spatial resolution particularly at long drift distances since the effective number of electrons $N_{\rm eff}$ [8, 15–19], which determines the azimuthal spatial resolution of a pad row, is approximately proportional to the average number of drift electrons collected by the pad row.

We present the electron transmission rate of a real-size gating foil measured using an ^{55}Fe source and a laser for a wide range of the voltages applied across the foil (ΔV) in the absence of a magnetic field. The upper limit of the transmission rate for (or the lower limit of the blocking power against) positive ions in the presence of a magnetic field is then estimated from the measured electron transmission with a reverse bias (negative ΔV). This paper is a digest version of a full paper. The interested reader is referred to Ref. [20] for further details with all relevant figures, pictures and a complete list of references.

2. Gating foil

The gating foil was fabricated by Printed Circuit Technology R&D Department of Fujikura Ltd. using dedicated flexible printed-circuit production techniques in order to realize a thin GEM-like structure having hexagonal holes with narrow rims. See Ref. [21] for the technical details of the production process.

The size of the nearly trapezoidal effective area is $\sim$ 143 mm $\times$ (211 mm – 232 mm), which fits in our prototype of the ILD-TPC readout module. The hole pitch is 335 µm and the rim width is $\sim$ 26 µm ($\sim$ 31 µm) on the front (back) side, yielding an optical aperture ratio of $\sim 82\%$. Magnified photos of the foil are shown in Fig. 1 while Fig. 2 shows the cross section of the rim. The typical error of the dimensions shown in the figures is $\lesssim \pm 1$ µm.

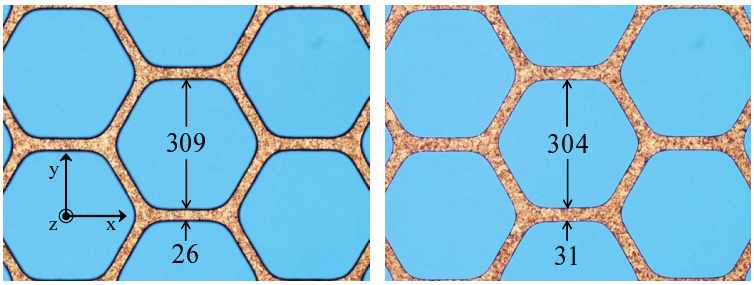

Figure 1. Magnified photographs of the effective area of the gating foil: the left (right) panel for the front (back) side, with dimensions in microns.

3. Experimental setup and data taking

3.1. Setup

The experiment was conducted after the measurement of the avalanche fluctuation [22] with essentially the same setup using a test chamber box for the prototype readout module of the ILD-TPC, and a radiation source: an ^{55}Fe source or a laser. Only the amplifier and the digitizer (modified ALTRO readout system) were replaced with the combination of a charge-sensitive preamplifier (ORTEC 142PC), a shaper amplifier (ORTEC 672), and a CAMAC peak-sensitive analog-to-digital converter module (Hoshin ADC C008).

The readout plane is paved over with 28 pad rows (5.26 mm wide), each consisting of small pads arranged at a pitch of $\sim$ 1.2 mm. The signal charges on the anode pads located at the

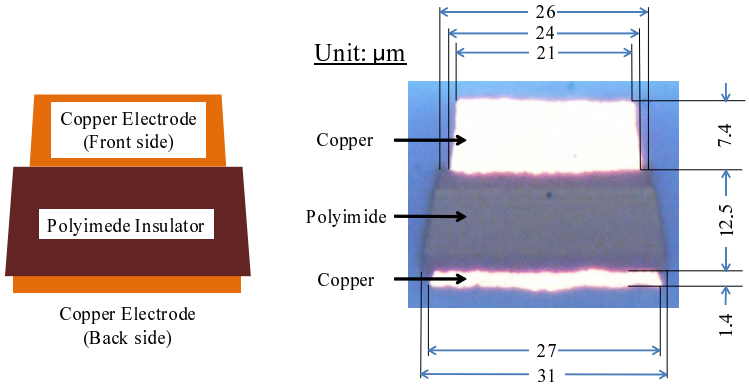

Figure 2. Cross-section of the hexagonal rim in the effective area of the gating foil: a schematic view (left) and a photomicrograph with the typical dimensions (right).

area under study are summed on the corresponding connector (central connector), and then sent to a preamplifier located nearby via a coaxial cable. Thus, the signal charge is measured on a connector-by-connector basis, instead of a pad-by-pad basis in the previous experiment. Each connector reads out signals on 32 pads in contiguous two pad rows, covering an area of $\sim$ 11 mm $\times$ 19 mm on the pad plane. In the measurement with the ^{55}Fe source the analog sum of the charges on the adjacent connectors is also recorded in order to select off-line the events in which most of the charge is collected on the central connector. The gating foil is placed on top of the double GEM stack with a gap of 9.4 mm. The gap is referred to hereafter as the transfer region.

In the measurement with the laser (New Wave Research Polaris II), a pulsed UV beam (λ = 266 nm) is injected into the chamber box, located at the laser focal point, through a quartz window. Electrons are created along the beam by two-photon ionization processes and detected by the pad rows arranged normally to the beam after gas amplification.

The filling gas is a premix of Ar-CF_4(3%)-isobutane(2%) at atmospheric pressure and room temperature ($\sim$ 25°C). The high voltage applied across the first (second) stage GEM is 345 V (315 V) and the electric field in the transfer (induction) gap is 900 V/cm (2700 V/cm), yielding an effective gas gain of $\sim$ 3700. The electric fields in the drift region ($E_{\rm d}$) and the transfer region ($E_{\rm t}$) are both set to 230 V/cm. For details of the experimental setup, see Ref. [20].

3.2. Data taking

First, the electron transmission rate was measured with the ^{55}Fe source using the technique employed in Ref. [12]. A set of runs, one with the normal drift field (normal run) and the other with the reversed field (reverse run), was repeated for each voltage across the gating foil (ΔV). The normal run gives the pulse height distribution for the photons converted in the drift region (gated signals) as well as for those converted in the transfer region (ungated signals) while the reverse run provides the distribution only for the ungated signals. In the analysis, the distribution of the reverse run was subtracted from that of the normal run in order to obtain the precise photo-peak position for the gated electrons. This procedure was required especially when the transmission rate of the gating foil was high and the four peaks (including escape peaks) partially overlapped in the normal run. The data were taken for ΔV between -4.5 V and $+19.5$ V. The negative sign of ΔV indicates the electric field direction within the holes of the gating foil opposite to the drift field.

The transmission rate was measured for ΔV down to -15.5 V using the laser with a larger

number of liberated electrons. The laser beam could be injected only into the drift region, i.e. upstream of the gating foil in the present setup. Therefore, runs for the normalization of the transmission rates were necessary at ΔV where the transmission rate had been measured in the ^{55}Fe runs ($\Delta V = -0.5$ V).

The typical data taking time of each run was 10 minutes, corresponding to 12 000 laser shots. It was short enough to ensure the constant gas density, and therefore the gas gain of the GEM stack, during each run. See Ref. [20] for details of the data taking procedure.

4. Results

4.1. Measurement with ^{55}Fe source

Several examples of the pulse height spectra obtained in the ^{55}Fe runs are shown in Fig. 3. The electron transmission rates were obtained from the ratio of the photo-peak positions (the gated to the ungated) determined by Gaussian fittings after pedestal subtraction for -4.5 V $\leq \Delta V \leq +19.5$ V. The results are shown in Fig. 4 along with those obtained with the laser.

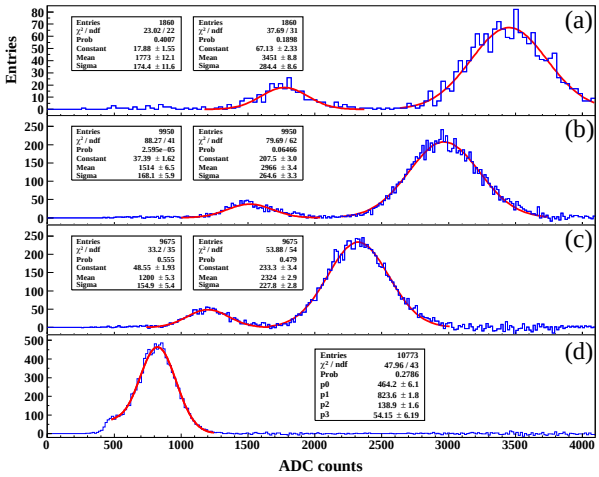

Figure 3. Examples of the pulse height distributions in the ^{55}Fe runs: (a) for the ungated signals, and (b), (c), (d) for the gated signals obtained respectively with $\Delta V = +3.5$ V, 0.0 V and -4.5 V, along with the fitted Gaussians. The pedestal is located around 110 ADC counts.

4.2. Measurement with laser

In the laser runs the charge only on the central connector was recorded. The typical number of electrons created along a laser-induced track was 1300 for a single connector (two pad rows). Examples of the pulse height distributions are shown in Fig. 5. The electron transmission rate for each ΔV was determined from the ratio of the peak position to that in the corresponding normalization run, for which the transmission rate had been measured to be $58.74 \pm 0.11\%$ using the ^{55}Fe source. The *peak* position was defined as the simple average of the pulse height distribution since it became skewed for low transmission rates because of the Poisson-like statistics of the small number of electrons passing through the gating foil.

The measurements were carried out from -0.5 V (for the normalization) down to -15.5 V. The results are shown in Fig. 4 along with those obtained by the ^{55}Fe runs. Also shown in the figure are the simulated transmission rates for electrons. The simulation was carried out using Garfield ++ (release v1r0) interlaced with Gmsh and Elmer. Fig. 6 shows an example of the electric field configuration in the proximity of the gating foil, given by the simulation.

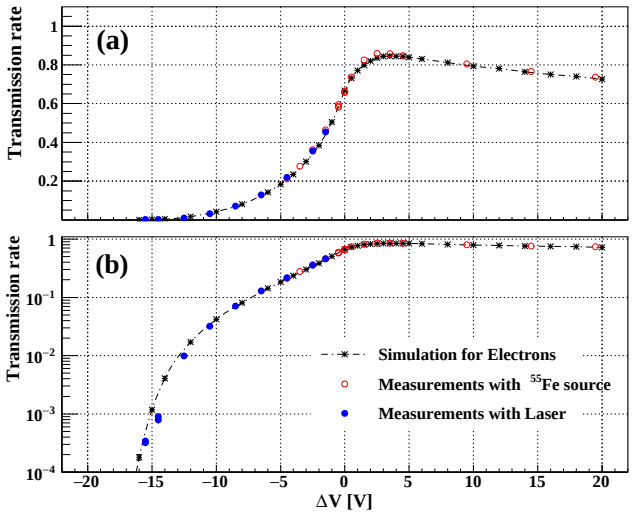

Figure 4. Measured electron transmission rate as a function of the bias voltage applied to the gating foil: (a) in linear scale, and (b) in log scale. Also shown in the figures are the measurements with the laser and the results of simulation (see Section 4.2).

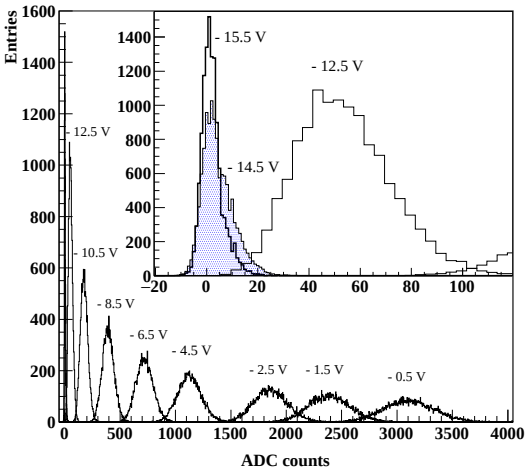

Figure 5. Examples of the pulse height distributions after pedestal subtraction obtained with the laser for different bias voltages (ΔV) on the gating foil. A magnified view in the inset shows some of those obtained with large reverse biases.

5. Discussion

The influence of a magnetic field is negligibly small for positive ions because of their large masses. Therefore, positive ions move closely along the electric field lines even under a high magnetic field. As a consequence, they drift like electrons in the reversed electric field and in the absence of a magnetic field. The transmission rate measured with negative ΔVs for electrons without magnetic field is hence expected to be larger than that for positive ions at the same ΔV under an axial magnetic field of 3.5 T because of (much) larger diffusion.

The upper limit of the transmission rate of the gating foil for positive ions is $(3.36 \pm 0.05) \times 10^{-4}$ at $\Delta V = -15.5$ V. The *blocking* power against positive ions is already sufficiently high.

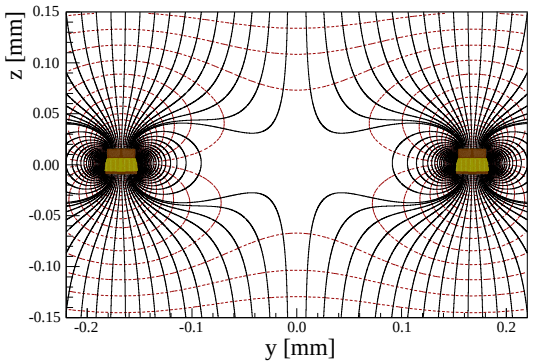

Figure 6. Electric field lines and equipotential lines around a hole in the gating foil placed in an otherwise uniform electric field of 230 V/cm, in the y-z plane at $x = 0$. See the left panel of Fig. 1 for the definition of coordinate system. The bias applied to the gating foil (ΔV) is -16.0 V.

The GEM stack (or Micromegas) is expected to be operated with an effective gas gain of $\sim$ 2000 in the real experiment. The number of outgoing positive ions per incoming drift electron is about 100, assuming a value of 5% for the value of IBF of our double GEM stack. Consequently, the number of positive ions drifting back to the drift volume is expected to be at most $100 \times 3.4 \cdot 10^{-4} = 0.034$ per incoming drift electron. In addition, the gating foil withstands larger negative ΔVs, down at least to -20 V. Therefore, the average number of back-drifting positive ions in the drift region is much smaller than that of primary ions, and so would be their influence on the drift field.

Under a high magnetic field, the motion of drift electrons is strongly restricted to the direction of the axial magnetic field. Therefore, the electron transmission rate under an axial magnetic field of 3.5 T is expected to be close to the optical aperture ratio of the gating foil ($\sim$ 82%) with ΔV around 0 V. See Ref. [20] for thorough discussions.

6. Conclusion

We have developed a real size gating foil to prevent secondary ions from entering the drift volume of the TPC for the international linear collider experiment. It is easy to be integrated in the modularized readout unit employing a micro-pattern gas detector (MPGD) for gas amplification.

Its transparency for drift electrons in a gas mixture of Ar-CF_4(3%)-isobutane(2%) was studied using an ^{55}Fe source and a UV laser for a wide range of the bias voltages applied across the foil, under a uniform electric field of 230 V/cm in the absence of a magnetic field.

The maximum electron transmission rate was measured to be about 86% at a forward bias voltage of $\sim +3$ V across the foil, whereas the minimum was $(3.36 \pm 0.05$ (stat. only)$) \times 10^{-4}$ at a reverse bias voltage of -15.5 V. The minimum transmission rate quoted above for the electrons is the upper limit of the transmission rate for positive ions at the same reverse bias voltage, even in the presence of a magnetic field. The blocking power of the gating foil against positive ions at ΔV = -15.5 V is high enough to keep the drift region of the MPGD-based ILD-TPC virtually free from the back-drifting ions created in the gas amplification device. The maximum electron transmission rate under a 3.5 T magnetic field is expected to be close to the optical aperture ratio of the foil (82%) with the foil unbiased.

Acknowledgments

We are grateful to Mr. S. Otsuka and Mr. S. Watanuki with Fujikura Ltd. for the development and production of the gating foils. We would like to thank the people with REPIC Corporation for the preparation of the experimental apparatus including the prototype readout module of the ILD-TPC. We would like also to thank colleagues of the ILD-TPC collaboration for their continuous support and encouragement. This work was partly supported by the Grant-in-Aid for Specially Promoted Research Grant No. JP23000002 of Japan Society for the Promotion of Science.

References

[1] Nygren D R 1974 Proposal to investigate the feasibility of a novel concept in particle detection (Lawrence Berkeley Laboratory (LBL) internal note)
URL `https://inspirehep.net/record/1365360`

[2] Sauli F 1997 *Nucl. Instrum. Methods Phys. Res.* A **386** 531

[3] Giomataris Y 1996 *Nucl. Instrum. Methods Phys. Res.* A **376** 29

[4] Behnke T *et al.* 2013 The international linear collider technical design report vol 4 `arXiv:1306.6329 [physics.ins-det]`

[5] Behnke T *et al.* 2013 The international linear collider technical design report vol 1–4
URL `https://ilchome.web.cern.ch/publications/ilc-technical-design-report`

[6] Ackermann K *et al.* 2010 *Nucl. Instrum. Methods Phys. Res.* A **623** 141

[7] Dixit M *et al.* 2007 *Nucl. Instrum. Methods Phys. Res.* A **581** 254

[8] Kobayashi M *et al.* 2011 *Nucl. Instrum. Methods Phys. Res.* A **641** 37

[9] Attié D *et al.* 2017 *Nucl. Instrum. Methods Phys. Res.* A **856** 109

[10] Adolphsen C *et al.* The international linear collider technical design report vol 3.II: Accelerator Baseline Design `arXiv:1306.6328 [physics.acc-ph]`

[11] Vogel A 2008 Beam-induced backgrounds in detectors at the ILC Ph.D. thesis Universität Hamburg
URL `http://www-library.desy.de/preparch/desy/thesis/desy-thesis-08-036.pdf`

[12] Sauli F, Ropelewski L and Everaerts P 2006 *Nucl. Instrum. Methods Phys. Res.* A **560** 269

[13] Gros P *et al.* 2013 *J. Instrum.* **8** C11023

[14] Ikematsu K 2014 Development of large-aperture GEMs as a gating device of the ILC-TPC for blocking positive ion feedback *Conf. Record IEEE Nuclear Science Symp. (Seattle)* N44-7

[15] Kobayashi M 2006 *Nucl. Instrum. Methods Phys. Res.* A **562** 136

[16] Arogancia D C *et al.* 2009 *Nucl. Instrum. Methods Phys. Res.* A **602** 403

[17] Kobayashi M 2013 *Nucl. Instrum. Methods Phys. Res.* A **729** 273

[18] Kobayashi M *et al.* 2014 *Nucl. Instrum. Methods Phys. Res.* A **767** 439

[19] Yonamine R *et al.* 2014 *J. Instrum.* **9** C03002

[20] Kobayashi M *et al.* 2019 *Nucl. Instrum. Methods Phys. Res.* A **918** 41

[21] Arai D 2018 Development of gating foils to inhibit ion feedback using FPC production techniques *EPJ Web of Conferences* **174** 02007 Proc. the 4th Conf. on Micro-Pattern Gaseous Detectors (MPGD 2015, Trieste)
URL `https://doi.org/10.1051/epjconf/201817402007`

[22] Kobayashi M *et al.* 2017 *Nucl. Instrum. Methods Phys. Res.* A **845** 236